Indian Journal of Chemistry
Vol. 63, March 2024, pp. 325-331
DOI: 10.56042/ijc.v63i3.6996

Oxidative decolorization of Mordant Black 17 by peroxydisulfate facilitated by Fe^{2+}

Abhishek Srivastava*[a], Neetu Srivastava[b] & Ruchi Singh[c]

[a] Department of Chemistry, GLA University, Mathura 281 406, U.P., India

[b] Department of Chemistry, D.D.U. Gorakhpur University, Gorakhpur 273 001, U.P. India

[c] Department of Chemistry, B. N. College of Engineering and Technology, Lucknow 226 201, U.P., India

E-mail: aabhichem@gla.ac.in

Received 28 November 2023; accepted(revised) 22 February 2024

The present study focuses on investigating the decolorization of Mordant Black17 (MB17) in aqueous solutions using peroxydisulfate. The impact of the initial dye concentration, as well as the concentrations of peroxydisulfate and Fe^{2+}, temperature, and *p*H on the decolorization of MB17 has been investigated. The experimental data have been examined employing kinetics of both first and second order. The decolorization kinetics of MB17 in the peroxydisulfate process adhered to the principles of second-order reaction kinetics, with a rate constant of 2.75×10^{-4} M^{-1} min^{-1} at 3.0 mM $S_2O_8^{2-}$ concentration. Decolorization efficiency above 93% has been achieved in 120 minutes under optimal reaction conditions. The rate constants pertaining to the second-order chemical process demonstrate a positive association with both $S_2O_8^{2-}$ concentration and temperature. Fe^{2+} activates $S_2O_8^{2-}$ to generate sulfate radical ion, amplifying MB17 decolorization. At higher *p*H, sulfate-free radical production decreases, limiting MB17 decolorization. Peroxydisulfate decolorized MB17 with a low activation energy of 45.36 kJ mol^{-1} at 3.0 mM starting concentration. The positive ΔG value indicates the non-spontaneity of the decolorization process.

Keywords: Peroxydisulfate, Mordant Black17, Decolorization, Kinetics, Activation parameters

Water pollution is a significant and enduring challenge that has plagued human society across the ages. Its detrimental impact on the health and well-being of billions of individuals globally is undeniable, leading to the emergence of many diseases including cholera, diarrhoea, and cancer[1,2]. Moreover, water pollution has been linked to adverse effects on vital organs such as the skin, lungs, brain, kidneys, and liver[1,2]. A plethora of infectious and harmful contaminants, such as radioactive elements, heavy metal ions, dyes, and pesticides, can be found in copious quantities of wastewater[3, 4]. The primary contributors to wastewater contamination are organic dyes derived from paper, pulp, leather, food, pharmaceuticals, textiles, paints, and coating industries[5, 6]. Cost-effective and efficient procedures and techniques are crucial for the removal of hazardous dyes from wastewater due to their significant implications for public health and the preservation of aquatic ecosystems[7]. In order to effectively eliminate dyes from aqueous solutions and wastewater, numerous methodologies have been commonly utilized, encompassing adsorption, coagulation, microfiltration, nano-filtration, photo-catalysis, ozonation, electrochemistry, aerobic and anaerobic microbial degradation, membrane separation, oxidative degradation, and chemical oxidation[8-13].

World Health Organization (WHO) reports that 17-20% of industrial water contamination stems from textile dyeing processes. About 80% of azo dyes are utilized in textile dyeing, and 10-15% are lost through wastewater without binding to fiber[14,15]. The ineffective degradation performance of azo dyes by conventional biochemical treatments can be attributed to the presence of azo bonds and aromatic rings within their structure[16]. The synthetic dyes must be non-selectively oxidized using degradation technologies; however, conventional methods have drawbacks such as insufficient mineralization, protracted treatment periods, sludge production, and the necessity for regeneration[17]. Advanced oxidation processes (AOPs) have been extensively investigated for the non-selective degradation of azo dyes. AOPs encompass the methodologies reliant on oxidizing agents such as Fenton's reagent, persulfate, and hydrogen peroxide, in addition to irradiation techniques like ultrasound and UV[18-21].

Fenton-type technologies generate potent oxidizing species such as hydroxyl radicals (˙OH) which target dye molecules[22]. Sulfate radical-based AOPs have emerged as highly promising methods for treating recalcitrant pollutants in recent times[23]. Like hydroxyl radicals (E_o = 2.8V), sulfate radicals (E_o = 2.5-3.1 V) can oxidize azo dyes into tiny molecules and carbon dioxide[24]. In terms of longevity, sulfate radicals exhibit a comparatively extended survival period in comparison to hydroxyl radicals[25-27]. Peroxydisulfate, being a potent supplier of sulfate radicals, exhibits notable merits such as remarkable aqueous solubility and exceptional stability under ambient conditions[19, 21]. Peroxydisulfate reactions are generally sluggish at room temperature, the persulfate activation strategies embrace a variety of techniques, including the utilization of transition metals (*e.g.*, Cu, Fe, and Ag), UV radiation, ultrasonic waves, alkali substances, thermal activation and activated carbon[28-34].

$$S_2O_8^{2-} \xrightarrow{\text{Heat}} 2\,SO_4^{-\bullet} \quad \ldots (1)$$

$$S_2O_8^{2-} \xrightarrow{\text{UV light}} 2\,SO_4^{-\bullet} \quad \ldots (2)$$

$$S_2O_8^{2-} \xrightarrow{\text{Ultrasonication}} 2\,SO_4^{-\bullet} \quad \ldots (3)$$

$$S_2O_8^{2-} + Fe^{2+} \longrightarrow SO_4^{-\bullet} + SO_4^{-} + Fe^{3+} \quad \ldots (4)$$

$$2S_2O_8^{2-} + 2H_2O \xrightarrow{OH^-} SO_4^{-\bullet} + 3SO_4^{-} + 4H^+ + O_2^{\bullet} \ldots (5)$$

Within the realm of advanced oxidation processes, it has been observed that homogeneous AOPs utilizing persulfate exhibit remarkable efficacy in the degradation of dyes and pollutants. This is attributed to the generation of sulfate ions as the end product, which are inert and environmentally benign[21].

Mordant Black17 (MB17) (Fig. 1) is an azo dye that has gained prominence in industrial settings due to its notable applications. MB17 is extensively employed in the dyeing process of wool, silk, and polyamide fabrics[35, 36]. MB17 was selected as a prototype dye for our mineralization investigations due to its inclusion of aromatic rings, which pose challenges for conventional treatment methods[37]. The oxidative degradation of aromatic rings by $S_2O_8^{2-}$ ions exhibits a high degree of sensitivity to the reaction conditions, *p*H value of the solution, and monomeric structure[21]. Photocatalytic and electrochemical methodologies were employed by a diverse group of scientists to facilitate the degradation of azo-based dyes[38-40]. Peroxydisulfate and various Fenton's reagents, either alone or in conjunction with a catalyst or ultrasonication, have demonstrated significant efficacy in the decolorization of acidic azo dyes[41, 42].

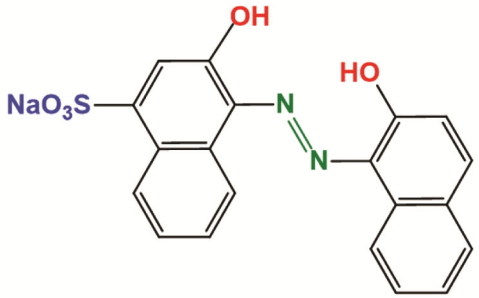

Fig. 1 — Molecular structure of Mordant Black 17 (MB17)

To the best of our understanding, there have been limited endeavours undertaken to explore the kinetics and thermodynamic analyses of the peroxydisulfate process. This research proposes the utilization of potassium peroxydisulfate as a means to decompose MB17. This paper presents and discusses the findings of studies conducted on the impact of [$S_2O_8^{2-}$], initial MB17 concentration, temperature, and *p*H value on the process of color removal. The experimental results were subjected to analysis employing both first and second-order kinetics. The parameters that define the characteristics of each model have been established. The objective of this study is to ascertain the optimal operating parameters for the disintegration of acid azo dyes, which will be consistent with investigations on real wastewater treatment.

Materials and Methods

Reagent Used

All experiment was conducted using double-deionized water and analytical-grade reagents over the entire study. Mordant Black17 (MB17) utilized (Tokyo Chemical Industry, India) was of utmost purity. Himedia India supplied $K_2S_2O_8$ (99.9%), and $FeSO_4.5H_2O$ (99.5%) which were utilized without subsequent purification. H_2SO_4 (Merck, India) and NaOH (Fisher Scientific, India) were employed to modulate the *p*H of the reaction medium.

Instrumentation

The *p*H of the solution under investigation was monitored using a DD LAB (model LAB.PHM.66800620) digital *p*H meter, which had been properly calibrated with a specified buffer solution. The absorbance at a specific wavelength of 570 nm was

measured utilizing an Electronics India model 2375 double-beam UV-visible spectrophotometer.

Experimental procedure

A batch reactor was employed in the experiment, utilizing a 250 ml three-necked stoppered round bottom glass vessel. The degradation of MB17 was investigated by a series of batch studies, wherein a solution of $K_2S_2O_8$ was introduced into a reactor holding the MB17 solution. The solution containing Fe^{2+} ions was rapidly mixed with MB17. The *p*H of each solution was regulated by 0.1 M H_2SO_4 or 0.1 M NaOH. The resultant reaction mixture was subjected to a water bath maintained at a consistent temperature. The requisite amounts of dye solution were extracted from the reactor on a regular basis, and MB17 oxidation was examined by measuring the decrease in absorbance at 570 nm[35]. The determination of MB17 concentration in solution at various time points was accomplished by quantifying the absorbance at 570 nm, while the decline of decolorization was calculated using the previously established calibration curve.

The efficiency of color removal (η) was calculated through the utilization of the following formula:

$$Precentage\ Removal\ (\eta) = \frac{C_t - C_o}{C_o} \times 100 \quad \ldots (6)$$

where C_t and C_o represent the MB17 concentration at reaction time t and the initial concentrations, respectively.

The decolorization kinetics of MB17 through $S_2O_8^{2-}$ were examined using first and second-order reaction kinetics. The individual expression was depicted as follows:

For first-order kinetics,

$$ln\frac{C_o}{C_t} = k_1\, t \quad \ldots (7)$$

For second-order kinetics,

$$\frac{1}{C_t} - \frac{1}{C_o} = k_2\, t \quad \ldots (8)$$

Here k_1 and k_2 are the rate constant of the first-order and second-order kinetic equation respectively.

Results and Discussion

Effect of $[S_2O_8^{2-}]$

In the decolorization process, the initial concentration of $S_2O_8^{2-}$ is of utmost significance as it serves as a pivotal precursor for the production of reactive free radicals. The impact of varying peroxydisulfate dosage on the decolorization of MB17 was investigated under different initial $[S_2O_8^{2-}]$, while maintaining the *p*H at 2.5 and initial dye concentration at 2.0 ppm (Fig. 2). By augmenting the initial concentration of $S_2O_8^{2-}$ from 0.75 mM to 6.0 mM, a potential enhancement in the decolorization of MB17 from 74.7% to 91.5% was witnessed within a reaction time of 120 minutes. This observation is consistent with the findings of other investigated reactions[19-22]. The aforementioned observations can be elucidated by the supplementary generation of $HO^{\cdot}$(Eq. 9)[43]. Sulfate ($SO_4^{\cdot-}$) and hydroxyl ($HO^{\cdot}$) radicals initiate an attack on the structure (aromatic ring) of MB17 dye, resulting in the decolorization and/or mineralization of MB17 into carbon dioxide (CO_2) and water (H_2O) (Eq. 10). MB17 underwent decolorization through the destruction of the azo group (-N = N-), followed by complete mineralization[43].

$$SO_4^{\cdot-} + H_2O \longrightarrow HSO_4^- + OH^{\cdot} \quad \ldots (9)$$

$$AO7 + SO_4^{\cdot-}/OH^{\cdot} \longrightarrow \text{Oxidation Products } (CO_2 + H_2O) \quad \ldots (10)$$

The outcomes of a regression analysis for the decolorization of MB17 by peroxydisulfate, which was performed using first and second-order reaction kinetics, are depicted in Fig. 3 and 4, respectively. The observed values for the second-order and first-order rate constants were found to vary between 1.30–4.56×10^{-4} M^{-1} min^{-1}, and 0.0136-0.0254 min^{-1},

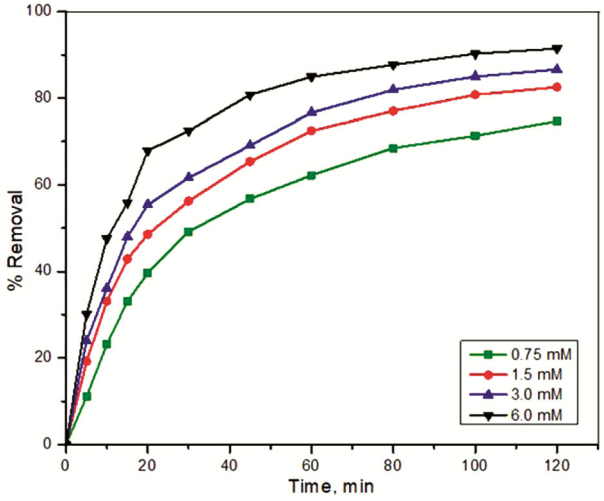

Fig. 2 — Influence of $S_2O_8^{2-}$ concentration on % removal of MB17 at [MB17] = 2.0 × 10^{-6} M, *p*H = 2.5 ± 0.1, Temp = 303 ± 0.1 K, and $[Fe^{2+}]$ = 2.5 × 10^{-4} M

respectively. Upon comparing the outcomes of the regression coefficients, it is observed that R^2 exhibited a value of 0.99 when considering the second-order reaction kinetics. Conversely, when considering the first-order reaction kinetics, R^2 displayed a value of 0.73. These findings indicate that the decolorization kinetics of MB17 adhere to the principles of second-order kinetics. The observed trend in the k_2 value demonstrated a direct correlation with the progressive augmentation of the initial concentration of potassium peroxydisulfate (Fig. 5). Analogous findings were likewise acquired through previous investigations[21].

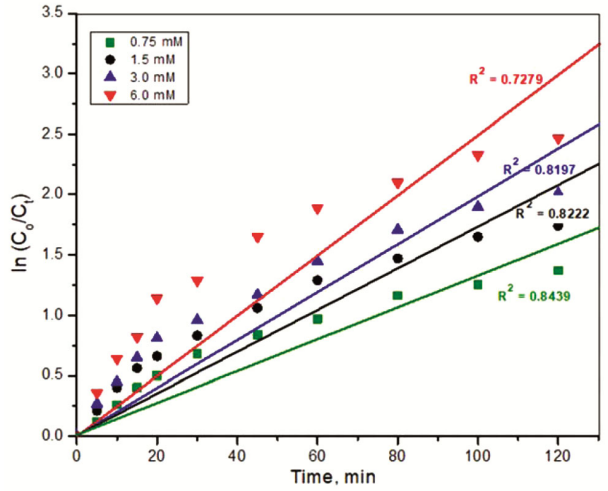

Fig. 3 — First-order reaction kinetics for decolorization of MB17 by $S_2O_8^{2-}$ at [MB17] = 2.0×10^{-6} M, *p*H = 2.5 ± 0.1, Temp = 303 ± 0.1 K, and $[Fe^{2+}] = 2.5 \times 10^{-4}$ M

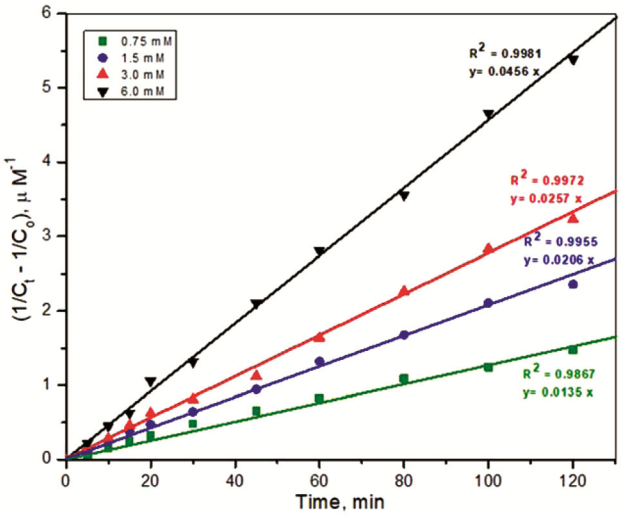

Fig. 4 — Second-order reaction kinetics for decolorization of MB17 by $S_2O_8^{2-}$ at [MB17] = 2.0×10^{-6} M, *p*H = 2.5 ± 0.1, Temp = 303 ± 0.1 K, and $[Fe^{2+}] = 2.5 \times 10^{-4}$ M

Effect of initial dye concentration

Fig. 6 illustrates the impact of varying initial concentrations (2.0, 4.0, and 8.0 ppm) of MB17 on the efficiency of decolorization. It has been discovered that there is a decrease in decolorization when the initial concentration of MB17 increases (Fig. 6). The efficiency of decolorization decreases from 87.2% to 42.5% when the concentration of MB17 increases from 2.0 to 8.0 ppm.

The decrease in decolorization efficiency can be attributed to the comparatively low concentration of free active radicals, which occurs as dye concentrations increase. At elevated levels of initial

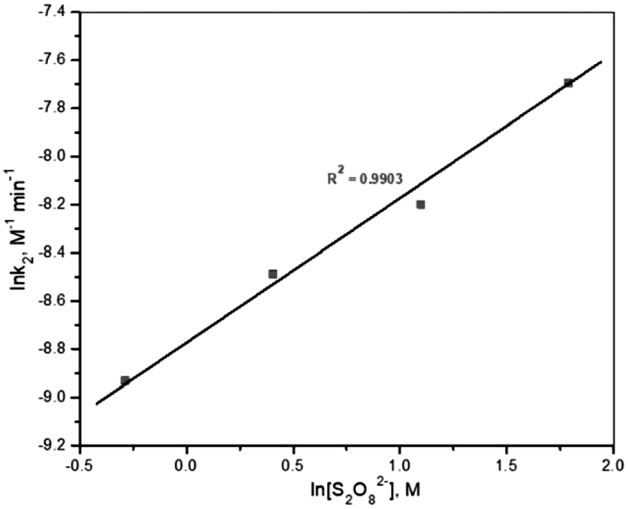

Fig. 5 — Influence of initial $S_2O_8^{2-}$ concentration on the second-order rate constant at [MB17] = 2.0×10^{-6} M, *p*H = 2.5 ± 0.1, Temp = 303 ± 0.1 K, and $[Fe^{2+}] = 2.5 \times 10^{-4}$ M

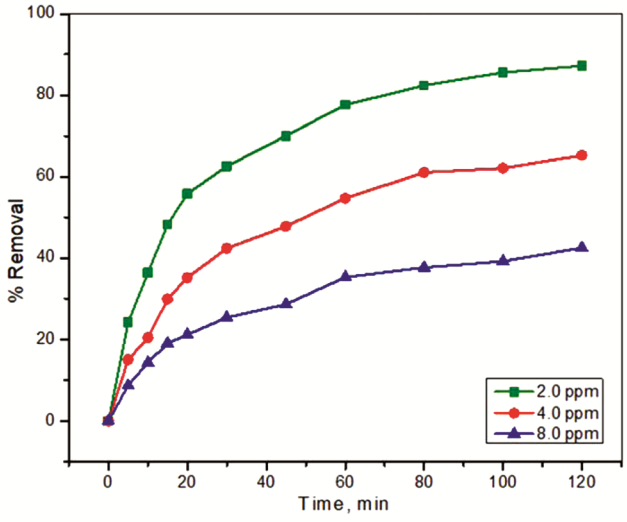

Fig. 6 — Influence of MB17 concentration on % removal of MB17 at $[S_2O_8^{2-}]$ = 3.0 mM, *p*H = 2.5 ± 0.1, Temp = 303 ± 0.1 K, and $[Fe^{2+}] = 2.5 \times 10^{-4}$ M

dye concentration, it is plausible that an increased quantity of free radical scavengers could be generated. Furthermore, the competition between the carbonaceous entities and free radical scavengers for free radicals would intensify due to the nonselective reactivity exhibited by free radicals[21]. Based on the aforementioned factors, it is plausible to infer that the efficacy of color removal may experience a decline when the initial concentration of MB17 is augmented.

Effect of *p*H

Prior studies on the oxidation of dyes, whether catalyzed or uncatalyzed, utilizing $S_2O_8^{2}$, have provided insights into the importance of *p*H in controlling the oxidation rate[19-22]. Table 1 displays the second-order rate constant (k_2) values pertaining to the oxidation of MB17 by $S_2O_8^{2-}$ at different *p*H levels. The degradation of MB17 was shown to be highest at a *p*H of 1.5 and thereafter decreased as the *p*H increased. Equations (11) and (12) demonstrate that the process of acid-catalysis can generate additional sulfate radicals, which will react with MB17 and enhance the effectiveness of degradation. Protons facilitate the generation of sulfate free radicals under acidic circumstances[44].

Table 1 — Influence of *p*H on the second-order rate constant Experimental Condition: [$S_2O_8^{2-}$] = 3.0 mM, [MB17] = 2.0×10^{-6} M, Temp = 303 ± 0.1K, and [Fe^{2+}] = 2.5×10^{-4} M

*p*H	$k_2 \times 10^4$, M^{-1} min^{-1}	R^2
1.5	3.28	0.992
2.5	2.75	0.997
3.5	2.56	0.993
5.0	2.39	0.990
6.0	2.23	0.995
7.0	2.08	0.991

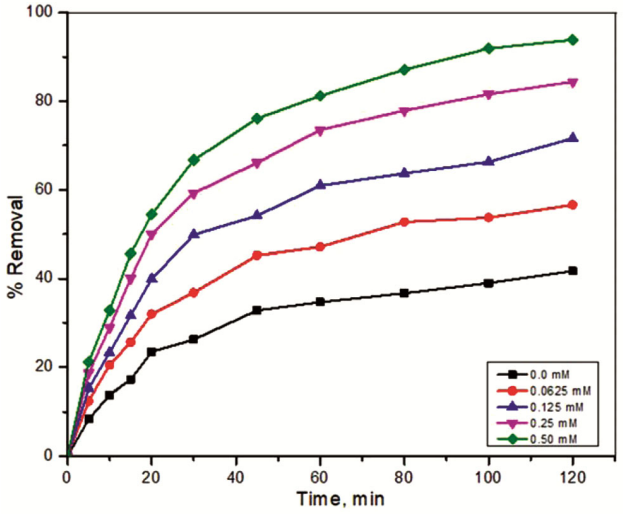

Fig. 7 — Influence of Fe^{2+} concentration on % removal of MB17 at [$S_2O_8^{2-}$] = 3.0 mM, [MB17] = 2.0×10^{-6} M, *p*H = 2.5 ± 0.1, and Temp = 303 ± 0.1 K

$$S_2O_8^{2-} + H^+ \longrightarrow HS_2O_8^- \quad \text{... (11)}$$

$$HS_2O_8^- \longrightarrow SO_4^{2-} + SO_4^{\bullet-} + H^+ \quad \text{... (12)}$$

$$SO_4^{\bullet-} + OH^- \longrightarrow SO_4^{2-} + OH^{\bullet} \quad \text{... (13)}$$

Increasing *p*H can convert sulfate radicals to hydroxyl radicals *via* reaction with OH^-(Eq. 13). In an aqueous solution, hydroxyl radicals react poorly with MB17. Thus, OH^- may scavenge MB17 degradation in alkaline solutions. In an alkaline milieu, the hydroxide ion exhibits scavenging properties towards sulfate radicals, thereby retarding the degradation reaction. Acidic conditions are more conducive to MB17 *in situ* oxidation. At elevated *p*H levels, the presence of Fe^{2+} may lead to the formation of a complex, hence impeding the production of sulfate radical ions[28]. This finding aligns with previous studies on the degradation of dyes employing peroxydisulfate.

Effect of [Fe^{2+}]

The Fe^{2+} is the chemical entity capable of catalyzing the activation of the $S_2O_8^{2-}$, resulting in the generation of reactive sulfate radical ion (Eq. 4). In order to investigate the impact of Fe^{2+}concentration of decolorization of MB17, its concentration was varied from 0.625×10^{-4} M to 5.0×10^{-4} M at 303 K temperature, while fixing MB17 concentration at 2.0×10^{-6} M, *p*H at 2.5, $S_2O_8^{2-}$concentration at 3.0mM. A potential increase in the decolorization of MB17 from 56.3% to 93.9% was noticed during a reaction time of 120 minutes by increasing the concentration of Fe^{2+} from 0.625×10^{-4} M to 5.0×10^{-4} M. In contrast, only 41.7% degradation of MB17 occurs in the absence of Fe^{2+} (Fig. 7). The experimental findings elucidate that the presence of Fe^{2+} exerts a synergistic effect on the decolorization of MB17 by promoting the generation of sulfate radical ion through the activation of $S_2O_8^{2-}$.

Effect of Temperature

The impact of temperature on the bleaching of MB17 was investigated at various temperatures (293 K, 303 K, 308 K, and 313 K). The experimental findings are depicted in Fig. 8. Increasing the temperature exerts a favorable influence on the

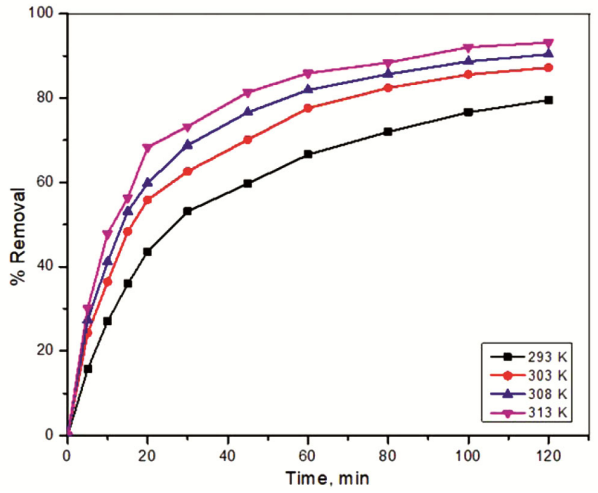

Fig. 8 — Influence of temperature on % removal of MB17 at $[S_2O_8^{2-}]$ = 3.0 mM, [MB17] = 2.0 × 10^{-6} M, *p*H = 2.5 ± 0.1, and $[Fe^{2+}]$ = 2.5 × 10^{-4} M

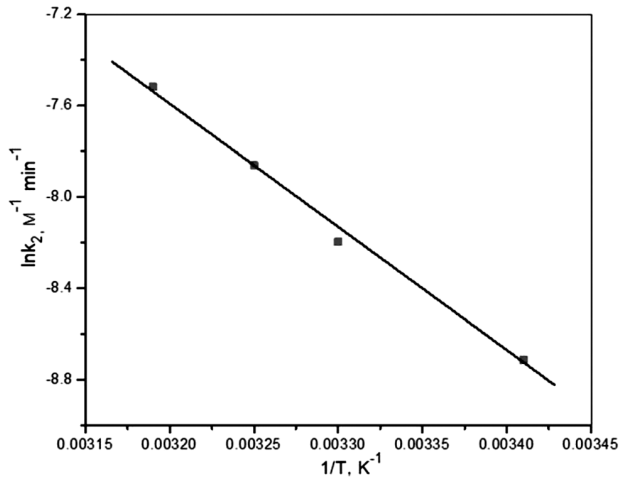

Fig. 9 — Arrhenius plot for decolorization of MB17 at $[S_2O_8^{2-}]$ = 3.0mM, [MB17] = 2.0 × 10^{-6} M, *p*H = 2.5 ± 0.15, and $[Fe^{2+}]$ = 2.5 × 10^{-4} M

Table 2 — Activation parameters for the degradation of MB17 by $S_2O_8^{2-}$ Experimental Condition: $[S_2O_8^{2-}]$ = 3.0 mM, [MB17] = 2.0 × 10^{-6} M, Temp = 303 ± 0.1K, *p*H = 2.5 ± 0.1, and $[Fe^{2+}]$ = 2.5 × 10^{-4} M

E_a kJ $mole^{-1}$	$\Delta H^{\#}$ kJ $mole^{-1}$	$\Delta S^{\#}$ J K^{-1} $mole^{-1}$	$\Delta G^{\#}$ kJ $mole^{-1}$
45.36	42.76	–173.37	93.51

process of decolorizing MB17. A temperature increase from 293 to 313 K resulted in a 79.5% to 93.2% improvement in decolorization efficiency. Furthermore, the duration for decolorization was significantly reduced due to the ability of peroxydisulfate to undergo accelerated decolorization at elevated temperatures. This phenomenon is attributed to the enhanced generation rate of sulfate free radicals, resulting in an intensified decolorization process for the dye.

By utilizing the Arrhenius and Eyring equations, the activation parameters were calculated. The plots of lnk_2 against the reciprocal of temperature exhibited a good linear relationship with R^2 = 0.99.At 3.0mM initial $S_2O_8^{2-}$ concentration (Fig. 9), the activation energy value was 45.36 kJ mol^{-1}. The findings indicate that the decolorization process generally advances with a low energy barrier. The experimental findings further demonstrated that the second-order kinetics exhibited a proportional augmentation of approximately 1.7-fold for every 10°C elevation (Table 2). The obtained results exhibit excellent concordance with previously documented literature pertaining to peroxydisulfate-mediated oxidation of azo dyes[21, 22].The ΔG value was positive, indicating that the degradation reactions exhibited non-spontaneity. In order to proceed with the reaction, a requisite amount of energy must be necessitated.

Conclusions

The process of oxidatively decolorizing MB17 using peroxydisulfate in an acidic environment was conducted and analyzed, both with and without a Fe^{2+} catalyst. The investigation encompassed the examination of various factors, such as peroxydisulfate concentration, MB17 concentration, *p*H level, concentration of Fe^{2+}, and temperature. Under the specified experimental conditions, a decolorization efficiency of over 93% was attained within a time frame of 120 minutes. The kinetic investigations revealed that the decolorization of MB17 exhibited kinetics consistent with second-order behavior. The rate constants associated with the second-order chemical reaction exhibited a positive correlation with both peroxydisulfate concentration and temperature. Fe^{2+} promotes MB17 decolorization by activating $S_2O_8^{2-}$ to generate sulfate radical ions. Due to the reduced generation of sulfate free radical at elevated *p*H, the rise demonstrates a decelerating influence on the decolorization process of MB17. Peroxydisulfate oxidation decolorized MB17 with an activation energy of 45.36 kJ mol^{-1} at 3.0 mM starting concentration.

References

1 Prakash S &Verma A K, *Int J Biol Innov*, 3 (2021) 38.
2 Dahiya V, *GSC Bio Pharm Sci*, 19 (2022) 205.
3 Sharma R, Agrawal P R, Kumar R &Gupta G, *Biosorption for Wastewater Contaminants*, Chapter 3, (John Wiley & Sons Ltd.) 2022, p. 42.

4 Yasasve M, Manjusha M, Manojj D, Hariharan N, Preethi P S, Asaithambi P, Karmegam N & Saravanan M, *Chemosphere*, 307 (2022) 136017.
5 Ardila-Leal L D, Poutou-Piñales R A, Pedroza-Rodríguez A M & Quevedo-Hidalgo B E, *Molecules*, 26 (2021) 3813.
6 Dassanayake R S, Acharya S &Abidi N, *Molecules*, 26 (2021) 4697.
7 Elgarahy A, Elwakeel K, Mohammad S & Elshoubaky G, *Chem Eng Technol*, 4 (2021) 100209.
8 Selvaraj V, Karthika T S, Mansiya C & Alagar M, *J Mol Struct*, 1224 (2021) 129195.
9 Ikram M, Zahoor M &Batiha G E S, *Z Fur Phys Chem*, 235 (2021) 1381.
10 Hamzezadeh A, RashtbariY, Afshin S, Morovati M &Vosoughi M, *J Env Anal Chem*, 102 (2022) 254.
11 Rathi B S. Kumar P S &Vo D V N, *Sci Total Env*, 797 (2021) 149134.
12 Kutluay S, *Fuel*, 287 (2021) 119691.
13 Goswami M K, Srivastava A, Dohare R K, Tiwari A K & Srivastava A, *Environ Sci Poll Res*, 30 (2023) 73031.
14 Sudha M, Saranya A &Selvakumar G, *Int J CurrMicrobiol App Sci*, 3 (2014) 670.
15 Baban A, Yediler A &Lienert D, *Dyes Pigments*, 58 (2003) 93.
16 Hassani A, Çelikdağ G, Eghbali P, Sevim M, Karaca S & Metin Ö, *UltrasonSonochem*, 40 (2018) 841.
17 Sarkar S, Banerjee A &Halder U, *Water ConservSciEng*, 2 (2017) 121.
18 Lee J, Von Gunten U & Kim J H, *EnvSci Tech*, 54 (2020) 3064.
19 Xu X R & Li X Z, *Sep Purif Tech*, 72 (2010) 105.
20 Wang P, Yang S, Shan L, Niu R & Shao X, *J EnvSci*, 23 (2011) 1799.
21 Ahmadi M, Behin J & MahnamA R, *J Saudi ChemSoc*, 20 (2016) 644.
22 Zhang H, Zhang J, Zhang C, Liu F & Zhang D, *UltrasonSonochem*, 16 (2009) 325.
23 Rastogi A, Al-Abed S R & Dionysiou D D, *ApplCatal B*, 85 (2009) 171.
24 Gayathri P, PraveenaJuliyaDorathi R & Palanivelu K, *UltrasonSonochem*, 17 (2010) 566.
25 Liu L, Yang C, Tan W & Wang Y, *ACS Omega*, 5 (2020) 13739.
26 Holkar C R, Jadhav A J, Pinjari D V, Mahamuni N M & Pandit A B, *J Env Manage*, 182 (2016) 351.
27 Matzek L W &Carter K E, *Chemosphere*, 151 (2016) 178.
28 Al-Thabaiti N S, AlSulami Q A &Khan Z, *J MolLiq*, 369 (2023) 20837.
29 Ewais H A,Basaleh A S &Al Angari Y M, *Int J ChemKinet*, 55 (2023)271.
30 Ji Q, Li J, Xiong Z & Lai B, *Chemosphere*, 172 (2017) 10.
31 Devi P, Das U & Dalai A K, *Sci Total Env*, 571 (2016) 643.
32 Boczkaj G & Fernandes A, *ChemEng J*, 320 (2017) 608.
33 Wang Z, Shao Y, Gao N, Lu X & An N, *Chemosphere*, 193 (2018) 602.
34 Ferkous H, Merouani S, Hamdaoui O & Petrier C, *UltrasonSonochem*, 34 (2017) 580.
35 Kodavatiganti S, Bhat A P & Gogate P R, *Sep PurifTechnol*, 279 (2021) 119673.
36 IIeri B, *EnvEng Res*, 27 (2022) 200287.
37 Panizza M & Cerisola G, *Water Res*, 43 (2009) 339.
38 Krishnakumar B & Swaminathan M, *SpectrochimActa Part A MolBiomol Spec*, 81 (2011) 739.
39 Yalcin S &Kara A J, *Nat App Sci*, 26 (2022) 115.
40 Chrystiane N B, Maiara B F, Suzana M L O M, Elaine C M M S, José J L L, Soliu O G&Carlos A M, *J ElectrochemSoc*, 165 (2018) 250.
41 Wawrzkiewicz M, Kotowska U & Sokół A, *Processes,* 9 (2021) 1911.
42 Lakshmi N J, Parag R &GogateAniruddha B P, *Pro Saf Env Pro*, 153 (2021) 178.
43 Aleboyeh A, Olya M E & Aleboyeh H, *Chem Eng J*, 137 (2008) 518.
44 Criquet J & Karpel V L N, *Chemosphere*, 77 (2009) 194.